Ultrasound scattering from silica fume clusters: in-line shear flow dynamics of hydrophilic or partially hydrophobic silica fume fillers in melts of non-polar polymeric systems

2008 J. Phys.: Condens. Matter 20 075105

(http://iopscience.iop.org/0953-8984/20/7/075105)

IOP Publishing Journal of Physics: Condensed Matter

J. Phys.: Condens. Matter **20** (2008) 075105 (12pp) doi:10.1088/0953-8984/20/7/075105

Ultrasound scattering from silica fume clusters: in-line shear flow dynamics of hydrophilic or partially hydrophobic silica fume fillers in melts of non-polar polymeric systems

Leïla Haïder[1], Jacques Tatibouët[1,3] and Laurent Ferry[2]

[1] Industrial Materials Institute (IMI), National Research Council Canada (NRC), 75 De Mortagne Boulevard, Boucherville, QC, J4B 6Y4, Canada

[2] Centre des Matériaux de Grande Diffusion, École des Mines d'Alès, 06 avenue de Clavières, 30319 Alès Cedex, France

E-mail: Jacques.Tatibouet@imi.cnrc-nrc.gc.ca

Received 26 September 2007, in final form 14 December 2007
Published 25 January 2008
Online at stacks.iop.org/JPhysCM/20/075105

Abstract

Shear flow dynamics of fractal aggregates are investigated by ultrasound scattering to study shear induced disruption processes of hydrophilic polydisperse silica fume fillers in melts of non-polar polymeric systems (polypropylene). A rheo-acoustical model in the low frequency scattering regime only involving structural parameters is proposed. Flow-dependent changes of the ultrasound scattering power per unit of volume from hydrophilic silica fume aggregates during extrusion are analyzed in the frame of the proposed rheo-acoustical model. In a second part, equilibrium structures of polymer coated silica fume fillers are investigated to elucidate the coupled intra- and inter-filler interactions. Surface chemistry of silica fume fillers was modified by grafting amphiphilic molecules with the same hydrophobic tail (long alkyl chains) and various hydrophilic polar heads (amine, carboxylic acid or hydroxyl groups) to obtain a range of hydrophobic fumed silica units. The effects of the surface layer of tethered chains and the extent of the coating level in a non-polar liquid dispersion are analyzed within the framework of the mismatch in chemical nature or solubility parameters between grafted chains and continuous polymer phase. Lastly, the ability of the ultrasound scattering technique to give a quantitative estimate of the critical disaggregation shear stress mainly representative of the particle surface adhesive energy in relation to filler surface modification is shown.

1. Introduction

The prediction of the acoustical properties of filled thermoplastic polymeric systems is a long standing problem of great interest in many industrial fields, especially for technological applications [1, 2]. Mixing is a key step in almost all polymer processing, affecting materials properties, processability and cost [1, 2]. Polymers are blended with other polymers to combine their properties and sometimes even to synergistically increase their physical characteristics [1–3]. Particulate fillers or reinforcing agents are widely used in the thermoplastics industry to enhance the mechanical performance of the finished composite, for example impact strength, high temperature creep resistance, stiffness and opacity, and further to impart specific properties to the mixture [1–3]. Interfacial interactions significantly influence the mechanical properties of the filled polymer since adhesion between particles and the polymeric matrix is mainly dependent upon both the size (area) of the interface and the strength of the interaction [1–3]. While the former quantity is related to the specific surface area of the

[3] Author to whom any correspondence should be addressed.

filler, the strength of the interaction can be altered by its surface modification [1, 2].

On the other hand, the ultrasound technique based on longitudinal propagation of acoustic waves provides a non-invasive and a powerful means for monitoring in-line polymeric materials processing and thus extracting mechanical properties of the probed materials during extrusion processes [4, 5]. During the past few years, fundamental and technological interests have been focused on either the time dependent isothermal measurements of the viscoelastic properties of the continuous polymer phase, crystallization kinetics, cross linking reactions or the dispersion state of the filled polymer [3–8]. The general goal in the former is to use the ultrasound technique as a basis of non-destructive evaluation of media that consist of a homogeneous isotropic continuous phase in which small particles are randomly dispersed. Ultrasonic wave propagation in such media is affected by loss of energy due to relaxation processes occurring in the continuous polymeric phase because of the viscoelastic properties of the rubber polymer and the scattering phenomenon at the filler particles [9, 10]. The scattering process mainly arises from the different modes of vibrations (radial pulsations or back and forth oscillations) in relation to either compressibility or density mismatches in the mechanical properties of continuous and particle phases [11]. Particle flocculation highly affects the low frequency scattering from a dense aggregate of size much smaller than the wavelength (Rayleigh scattering regime), which scales as the square of the cluster volume in dilute random dispersions [11]. Over the last two decades, most of the contributions have been directed towards a better understanding of the relationship between the ultrasonic scattering power and filler volume fraction under different flow conditions [12–14]. Little attention has been paid to the ultrasound scattering from a dense suspension of particles or clusters, which can no longer be considered as independent, and correlation effects influence the ultrasonic scattered power because of wavelet interference in a dense distribution of scatterers [15]. The low frequency scattered power per unit of volume can be considered as the result of imperfect wave destruction associated with either a packing factor [16–18] or the variance in local filler volume fraction [19, 20]. Primary particle size distribution further affects the scattering behavior, in the Rayleigh scattering regime, because of additional scattering arising from polydispersity [21, 22].

In the present paper, shear flow dynamics of fractal aggregates in melts of polymeric systems are investigated by ultrasound scattering. Under consideration of polydisperse weak Rayleigh scatterers with primary particle size distribution described by the gamma probability density function and considering the concept of variance in local filler volume fraction, we derive the original expression of the ultrasound scattering cross section per unit of volume for weak correlated Rayleigh fractal clusters. On the basis of the scaling laws for the shear break-up of the flocs, we propose a rheo-acoustical model only involving structural parameters for studying the shear stress dependence of the ultrasound scattered intensity from polydisperse fractal aggregates in dense systems.

The second section concerns in-line static and rheo-acoustical experiments for hydrophilic silica fume fillers, compounded in non-polar liquid medium (polypropylene) during extrusion to examine shear break-up processes of silica fume aggregates. Flow-dependent changes of the low frequency scattering power per unit of volume are analyzed on the basis of the proposed rheo-acoustical model.

Colloidal interactions between particles dispersed in a liquid can be suitably tailored by modifying the surface chemistry of the particles [23–31]. Coverage of the high energy surface of an inorganic filler with an organic substance results in a decrease of the free energy and induces the reduction in size of a cohesive minor component such as clusters of solid particles, which leads to a better surface quality of the final composite [23–31]. Surface chemistry of the silica fume particles covered with polar silanol groups was altered from hydrophilic to partially hydrophobic by grafting asymmetric amphiphilic molecules with the same hydrophobic tail (long alkyl chains) and various hydrophilic polar heads (amine, carboxylic acid or hydroxyl groups).

In section 3, the equilibrium structure of polymer coated silica fume fillers is investigated to elucidate the coupled intra- and inter-filler interactions and to give an understanding of the adsorbed polymer conformation. The effects of a surface layer of tethered alkyl chains and the extent of coating level are analyzed within the framework of the mismatch in solubility parameters between the grafted chains at the silica surface and the continuous polymer phase. Finally, the ability of the ultrasound scattering technique to give quantitative information on the filled polymeric matrix dispersion and to estimate the critical disaggregation shear stress representative of the particle surface adhesive energy in relation to filler surface treatment is further discussed.

2. Ultrasound scattering theory

We consider a homogeneous isotropic continuous polymeric matrix in which small particles are randomly distributed and probed by a longitudinal ultrasonic wave normally incident to the half space of scatterers. We further assume weakly scattering particles or aggregates of size small compared to the ultrasound wavelength λ, so that the Born approximation remains valid, and thus Rayleigh scattering theory can be used [11]. Theoretical models of ultrasound scattering are based on either the continuum [19, 20] or the particle approach [16–18]. The fundamental difference between the two lies in the manner in which the random medium is modeled. In each case, a linearized wave equation solved by the Green's function approach led to an integral expression of the scattered waves in terms of density and compressibility changes. Indeed, the continuum approach recognizes that particles separated by less than $\lambda/2$ cannot be resolved by the transducer and therefore the suspension can be modeled as a continuum medium in which local fluctuations in density and compressibility give rise to the scattered waves [19, 20]. In contrast, the particle approach tracks the position of every particle in the insonified region and sums the wavelets scattered from individual particles [16–18]. Recently, Mo

and Cobbold [32] introduced a new hybrid approach which sums the wavelets from elemental volumes or voxels of size $\approx\lambda/2\pi$ small enough that the incident wave arrives with the same phase at every particle located within it. In the low frequency scattering regime, the hybrid approach predicts a nearly isotropic scattered power scaling as the variance of the particle number in a voxel.

2.1. Random distribution of uncorrelated Rayleigh scatters

In random dilute dispersions, each uncorrelated particle, in the low frequency scattering regime, scatters the incident wave unaffected by the presence of the other particles. The directional ultrasonic scattering coefficient $\alpha_{\mathrm{m}}(\vec{\mathbf{k}},\vec{\mathbf{s}})$ defined as the power scattered per unit solid angle for an incident plane wave of unit amplitude, in the Rayleigh scattering regime, then scales as the inverse of the scattering mean free path l [34, 35],

$$\alpha_{\mathrm{m}}(\vec{\mathbf{k}},\vec{\mathbf{s}}) \approx \frac{1}{l} \tag{1}$$

with

$$l = \frac{1}{n\boldsymbol{\sigma}_{\mathrm{m}}(\vec{\mathbf{k}},\vec{\mathbf{s}})} \tag{2}$$

where $\vec{\mathbf{k}}$ and $\vec{\mathbf{s}}$ are respectively the incident and scattered wavenumber vectors, n is the average number of scatterers per unit of volume and $\sigma_{\mathrm{m}}(\vec{\mathbf{k}},\vec{\mathbf{s}})$ is the differential scattering cross sectional area of a weak Rayleigh scatterer of arbitrary shape of volume V and average size a, given by the Green's function approach [35]:

$$\sigma_{\mathrm{m}}(\vec{\mathbf{k}},\vec{\mathbf{s}}) \approx pV^2 \tag{3}$$

with

$$p = \pi^2 f^4 (\kappa_0\rho_0)^2 \times \left[\left(\frac{\kappa_{\mathrm{p}}-\kappa_0}{\kappa_0}\right) + \left(\frac{\rho_{\mathrm{p}}-\rho_0}{\rho_{\mathrm{p}}}\right)\frac{\vec{\mathbf{k}}\cdot\vec{\mathbf{s}}}{ks}\right]^2 \tag{4}$$

where f represents the ultrasound frequency and κ_{p}, κ_0 and ρ_{p}, ρ_0 are the compressibilities and densities of scatterer and suspending medium, respectively. In the Rayleigh scattering regime, the scattered power is proportional to the square of the particle volume and further scales as the fourth power of the ultrasound frequency.

Under consideration of polydisperse (continuous) distributions with primary particle size distribution (polydispersity) described by the gamma probability density function [21], whose skewness depends upon the normalized variance in size of the scatterers ($var(r) \equiv (\langle r^2\rangle - a^2)/a^2$), the differential scattering cross sectional area $\sigma_{\mathrm{p}}(\vec{\mathbf{k}},\vec{\mathbf{s}})$ satisfies the following relationship [8]:

$$\sigma_{\mathrm{p}}(\vec{\mathbf{k}},\vec{\mathbf{s}}) = \sigma_{\mathrm{m}}(\vec{\mathbf{k}},\vec{\mathbf{s}}) \times [(1+var(r))(1+2var(r))\ldots(1+5var(r))]. \tag{5}$$

The low frequency scattered power $\alpha_{\mathrm{p}}(\vec{\mathbf{k}},\vec{\mathbf{s}})$ per unit of volume from a random distribution of weak uncorrelated similarly shaped but differently sized scatterers thus becomes [8]

$$\alpha_{\mathrm{p}}(\vec{\mathbf{k}},\vec{\mathbf{s}}) \approx n\sigma_{\mathrm{m}}(\vec{\mathbf{k}},\vec{\mathbf{s}})(1+var(r)) \times (1+2var(r))\ldots(1+5var(r)). \tag{6}$$

Particle size distribution affects the ultrasonic scattering behavior of individual polydisperse scatterers and enhances the ultrasound scattering cross section per unit of volume because of additional scattering arising from polydisperse effects.

2.2. Random distribution of correlated Rayleigh scatters

In dense dispersion, the scatterers can no longer be considered independent since the increase in correlation among the polydisperse particles induces destructive interference of the far-field scattered waves and a decay of the scattered power for non-absorbing Rayleigh scatterers [16]. On the basis of the particle approach [17, 18, 21, 22], the low frequency scattering coefficient $\alpha_{\mathrm{p}}(\vec{\mathbf{k}},\vec{\mathbf{s}})$ can be evaluated by estimating the packing factor, which accounts for coherent addition of the scattered waves. The packing factor is contingent on the selection of an appropriate pair correlation depending on particle volume fraction, particle shape and flow conditions. The packing function viewpoint further involves some very complex statistical mechanics and provides unclear physical insight [21, 22]. One may thus consider an alternative approach [19, 32] based on the concept of variance in local filler volume fraction. The scattered power can then split into a part arising from a 'crystalline' phase which gives no net contribution because of destructive wave interference and another representing contributions from independent fluctuations in the particle number ω within the elemental voxel of volume ΔV and size $\approx\lambda/2\pi$. The low frequency scattered power from a dense distribution of weak correlated scatterers then scales as the variance $var(\omega) = \omega^2 - \bar{\omega}^2$ of the particle number ω within a voxel [19, 32, 33]:

$$\alpha_{\mathrm{p}}(\vec{\mathbf{k}},\vec{\mathbf{s}}) \approx \frac{1}{l} \qquad \text{with } l = \frac{1}{n\sigma_{\mathrm{p}}(\vec{\mathbf{k}},\vec{\mathbf{s}})(var(\omega)/\bar{\omega})} \quad \text{and } n = \bar{\omega}/\Delta V. \tag{7}$$

2.3. Correlated Rayleigh fractal clusters

Several models of random cluster growth developed in the last decade suggests that aggregates behave as fractals on a scale larger than the primary particle size. Computer simulation leads to self-similar clusters with radius of gyration obeying the scaling relationship [36, 37]:

$$R(N) \approx aN^{1/D} \tag{8}$$

where N is the number of particles in the fractal cluster, a the characteristic radius of elementary particles and D the fractal dimension of the clusters. A fractal dimension less than the Euclidean dimension d corresponds to open floc structures with porosity increasing with size.

Within the framework of a fractal flocculation process, ultrasound scattering from a weak Rayleigh cluster ($kR \ll 1$) is coherent and the differential scattering cross sectional area $\sigma_{\mathrm{ap}}(\mathbf{k},\mathbf{s})$ of a cluster of arbitrary shape of volume $V_{\mathrm{a}}(\bar{R})$ is mainly dependent upon both the particle number N within the fractal structure and the normalized variance in size $var(r)$ of the polydisperse scatterers:

$$\sigma_{\mathrm{ap}}(\vec{\mathbf{k}},\vec{\mathbf{s}}) \approx pV_{\mathrm{a}}^2(\bar{R})(1+var(r)) \times (1+2var(r))\ldots(1+5var(r)) \approx N^2\sigma_{\mathrm{m}}(\vec{\mathbf{k}},\vec{\mathbf{s}}) \times (1+var(r))(1+2var(r))\cdots(1+5var(r)). \tag{9}$$

In the case of monodisperse weak Rayleigh scatterers ($var(r) = 0$), the differential scattering cross sectional area

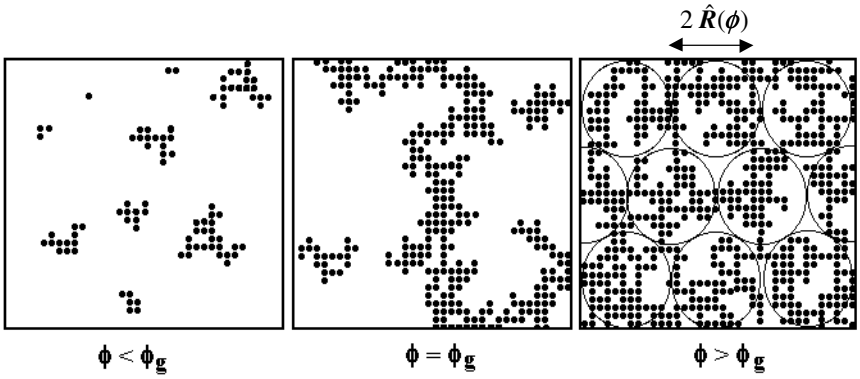

Figure 1. Structure of an aggregated suspension at rest ($\phi < \phi_g$, finite sized clusters; $\phi = \phi_g$, an infinite spanning cluster and some isolated aggregates; $\phi > \phi_g$, packing of fractal 'blobs' of size $\hat{R}(\phi)$) [38, 39].

$\sigma_{ap}(\vec{k}, \vec{s})$ then scales as the square of the particle number N within the fractal structure [$\sigma_{ap}(\vec{k}, \vec{s}) \approx N^2 \sigma_m(\vec{k}, \vec{s})$] [38, 39].

According to the hybrid approach model based on the concept of variance in local filler volume fraction, the ultrasonic scattering coefficient $\alpha_{ap}(\vec{k}, \vec{s})$ from weak polydisperse correlated Rayleigh aggregates satisfies the following relationship:

$$\alpha_{ap}(\vec{k}, \vec{s}) \approx \frac{1}{l_a} \qquad \text{with } l_a \approx \frac{1}{n_a \sigma_{ap}(\vec{k}, \vec{s})} \left(\frac{\bar{\omega}}{var_a(\omega)} \right) \quad (10)$$

where l_a is the scattering mean free path, $var_a(\omega)$ is the variance of the particle number ω in a voxel and $n_a = n/N$ the number of clusters per unit volume. Cluster growth increases the variance in particle number because each voxel can gain or lose a large number of elementary particles. At a first approximation, the variance $var_a(\omega)$ increases linearly with the volume fraction ϕ_a of the aggregates and can be reasonably approximated by the following expression [38, 39]:

$$var_a(\omega) \approx \frac{\phi_a}{\phi} var(\omega) \qquad \text{for } N \ll (ka)^{-D}. \quad (11)$$

We further define the normalized ultrasonic scattering coefficient $\alpha_r = \alpha_{ap}(\vec{k}, \vec{s})/\alpha_p(\vec{k}, \vec{s})$. Substituting for equations (9) and (11) in (10), with $\phi_a/\phi = (1/N)[V_a(\bar{R})/V]$, then gives the dimensionless ultrasonic scattering coefficient $\alpha_r(\vec{k}, \vec{s})$:

$$\alpha_r(\vec{k}, \vec{s}) = \left(\frac{R}{a} \right)^3 \qquad \text{for } kaN^{1/D} \ll 1. \quad (12)$$

The normalized ultrasonic scattering power $\alpha_r(\vec{k}, \vec{s})$ is nearly isotropic in the Rayleigh scattering regime and scales as the average volume $V_a(\bar{R})$ of clusters with no significant dependence upon the filler volume fraction or particle size distribution. Far field coherence effects and primary particle size distribution together determine the cluster volume dependence of the scattering coefficient $\alpha_r(\vec{k}, \vec{s})$. One can indeed expect no influence of the fractal dimension D of the clusters upon the volumetric scattered power per unit of volume α_r, because the ultrasonic transducer cannot resolve the internal structure of aggregates smaller than voxels. As a consequence, the dimensionless ultrasonic scattering coefficient $\alpha_r(\vec{k}, \vec{s})$ can be interpreted as an aggregation index in the low frequency scattering regime (Rayleigh scattering). In contrast, for clusters of size larger than the ultrasound wavelength ($kR \gg 1$), the hybrid approach is no longer valid because of angle dependent destructive interference [8, 38, 39]. In this case, a fractal scattering regime characterizes anisotropic structures [8, 38, 39]. The dimensionless ultrasonic scattering coefficient $\alpha_r(\vec{k}, \vec{s})$ mainly involves the scattering angle and fractal dimension of the clusters [8, 38, 39] and thus becomes sensitive to the internal structure of the aggregates and therefore to the polydispersity of the scatterers [8]. The normalized ultrasonic scattered power can no longer characterize the aggregation state of a suspension [8, 38, 39].

3. Rheo-acoustical model

In the dilute regime, the suspension only consists of isolated particles and finite sized particles. By increasing the particle volume fraction, clusters cannot indefinitely grow without interpenetration [40]. Above the percolation concentration ϕ_g, fractal structures then reach a maximum average size $\hat{R}$. In concentrated suspensions the infinite network may be considered as a collection of fractal subclusters of mean density $\hat{\phi}$ and size $\hat{R}(\phi) \approx a(\phi/\phi^*)^{1/D-3}$ packed with a volume fraction ϕ^* [40] (figure 1).

Above a critical yield stress, the shear thinning behavior of aggregated suspensions results from the rupture of the spanning network and finite clusters when increasing the shear stress. Clusters can grow in a shear field until they reach a maximum stable size corresponding to a dynamical equilibrium between formation and shear break-up of the aggregates [40]. An aggregate with radius above the maximum stable size is disrupted by shear stresses. As shown by experimental investigations [41] and computer simulations [42, 43], the shear stress dependence of the equilibrium radius $R(\tau)$ of an isolated fractal cluster obeys the

general power law relationship:

$$\frac{R(\tau)}{a} \approx \left(\frac{\tau^*}{\tau}\right)^m \qquad \text{with } 0.3 < m < 0.5 \qquad (13)$$

where the critical shear stress $\tau^* \approx \Gamma/a$ for cluster break-up is related to the surface adhesive energy Γ (adhesive energy per unit contact area) and the characteristic radius a of elementary particles. The break-up criterion $R^3(\tau) \approx CKa^2/\tau$ proposed by Potanin [42] involves an unknown fragility parameter C and the spring constant K of the bonds between particles. The fragility of bonds depends on the reversibility of cluster deformation under the action of external stresses [38, 40]. Soft and rigid clusters represent extreme possible behavior of the aggregates. Rigid clusters are more likely broken into secondary aggregates of approximately equal parts (*large scale fragmentation process*) since elastic deformations are transmitted over the whole structure [38, 40]. On the other hand, soft structures are irreversibly deformed by external stresses and splits of individual particles and small clusters one by one until the cluster reaches a stable size (*surface erosion process*) [38, 40].

One may thus consider the mean field approach proposed by Snabre *et al* [34, 40], giving a scaling law similar to the phenomenological equation (13) with $m = 1/2$ for deformable aggregates and $m = 1/3$ for rigid clusters, in good agreement with experimental investigations [41, 43] and computer simulations [42].

Considering both the cluster volume dependence of the scattered power per unit of volume and the scaling law for the shear break-up of the aggregates (power laws 12, 13), the shear stress dependence of the dimensionless ultrasonic scattering coefficient $\alpha_r(\tau)$ in the Rayleigh scattering regime only involves structural parameters and obeys the power law relationship

$$\alpha_r(\tau) = \left(\frac{R(\tau)}{a}\right)^3 \approx 1 + \left(\frac{\tau^*}{\tau}\right)^{3m} \qquad \text{for } (kR \ll 1) \quad (14)$$

where particle adhesiveness and cluster deformability respectively determine the critical shear stress τ^* for cluster break-up and the exponent m. In the Rayleigh scattering regime, particle volume fraction within the aggregates, particle size distribution and the fractal dimensionality have no influence upon the dimensionless ultrasonic scattering coefficient $\alpha_r(\tau)$.

4. Ultrasound scattering from silica fume aggregates

4.1. Properties of silica fume nanoparticles

Colloidal particles have long been used in a wide variety of applications to synthesize materials by controlling the aggregation or 'gelling' of the particles [44]. The molecular interactions found between these nanoparticles as they contact each other play the key role in the formation of bonds between the particles and control the ultimate nanoscale and macroscale organization of materials synthesized in this manner [44, 45]. Silica fumes are a by-product of silicon or ferrosilicon industry when produced in electric furnaces and has been widely employed as filler in silicon rubber-based products [46]. Furthermore, it is an extremely versatile material that can be used to modify the rheology of a variety of systems [23]. In addition, because of their potential application as composite polymer electrolytes in rechargeable lithium batteries [24], fumed silica particles have been used as a gelling agent in polar organic liquids [46–48]. In the present study, raw silica fume waste from a silicon plant (Péchiney Electrométallurgie-France) was used as fillers to increase the stiffness of thermoplastic polymers, especially polypropylene. Silanol groups (Si–OH) are generated on the silica surface during the preparation process [49]. When dispersed in liquid media, silica–silica interactions mainly involve silanol–silanol hydrogen bonding, giving rise to larger structures called flocs [46, 49]. At high fumed silica concentration, a three dimensional network of flocs extends throughout the volume sample and the suspension behavior is 'gel-like'. A network of bonded particles during the sol-to-gel transformation results from the creation of siloxane linkages (≡Si–O–Si≡) between the silica nanoparticles in the sol [46, 49]. Indeed, recent investigations by the atomic force microscopy (AFM) technique [50] have shown that adhesion between oxide surfaces such as silica nanoparticles is a mixture of hydrogen bonding (≡Si–OH···HO–Si≡), anionic hydrogen bonding (≡Si=$(OH)_2^-$ ···HO–Si≡) and covalent bonding via formation of siloxane (≡Si–O–Si≡). The formation of these bonds depends on the intrinsic silica surface composition, which varies with pH of the environment [50]. We used densified and non-densified hydrophilic silica fume nanoparticles with an average size of ≈50 nm and a specific surface area of 20 $m^2\ g^{-1}$ compounded in polypropylene homopolymer matrix (PP3400MA1 from APPRYL, melt flow index of 40 g/10 min) at 30 wt% loading. The main difference between the densified and non-densified fumed silica particles lies in the manner in which the treatment in the electric furnaces was performed.

4.2. Surface modification of silica fume nanoparticles

The effects of the tethered chains on colloidal particles have been extensively studied from the viewpoint of steric stabilization or the ability of the chains, usually polymeric, to provide thermodynamic stability of the particles in a dispersion [51–55]. Indeed, one of the methods for ensuring the aggregative stability of colloidal dispersions is their steric stabilization by a polymer bonded to the surface of the dispersed particles. This bonding is achieved by adsorption or by the grafting of macromolecules onto the surface. As a result, a protective layer is formed, thus preventing particle flocculation [54, 55].

Surface modification of non-densified hydrophilic silica fume nanoparticles was then carried out by grafting amphiphilic molecules onto the silica surface to obtain a range of hydrophobic silica units. For this purpose, asymmetric molecules with long hydrophobic tails composed of monoalkyl chains CH_3–$(CH_2)_{15}$–CH_2–NH_2 containing the polar amino group NH_2 (Akzo Nobel), CH_3–$(CH_2)_{15}$–COOH

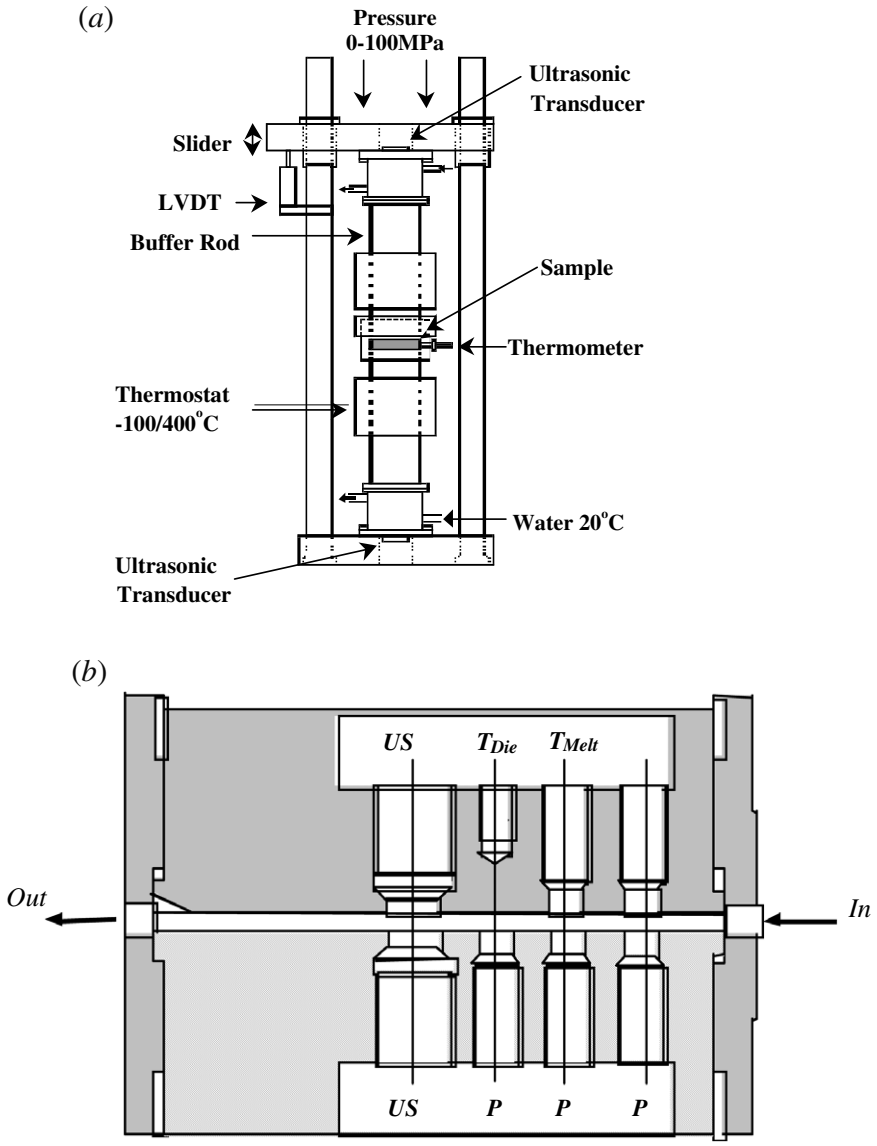

Figure 2. Experimental ultrasonic device in static mode (*a*) or instrumented die (*b*) with ultrasonic transducer (US), pressure probe (P), and both die and melt thermocouples (T_{die} and T_{melt}).

with the carboxylate acid group –COOH (Aldrich) or CH_3–$(CH_2)_{15}$–CH_2–OH having the hydroxyl functional group –OH (Aldrich) were then used. These molecules have little affinity for water because of the hydrophobic tail, and they have also little affinity for hydrocarbons because of the polar region. However, they will readily adsorb onto the particle surface, orientating themselves in such a way that the polar and non-polar parts are located in the most favorable environment [44]. Surface modification of densified hydrophilic silica fume nanoparticles was further performed by grafting monoalkyl CH_3–$(CH_2)_{16}$–NH_2, dialkyl CH_3–$(CH_2)_{16}$–NH–$(CH_2)_{16}$–CH_3 and methyl dialkyl amine CH_3–$(CH_2)_{16}$–NCH_3–$(CH_2)_{16}$–CH_3 onto the silica surface. Surface treatment of the hydrophilic silica fume particles was performed at 120 °C for one hour by dry blending in a high speed mixer (DRAIS EIRICH).

4.3. Ultrasonic experimental device

Ultrasonic experiments were first carried out in static mode [4] (figure 2(*a*)). The filled polypropylene (PP) with known thickness e was first confined between two aligned steel rods at the opposite end of which the ultrasonic transducers are attached. Ultrasonic properties of the confined polymer are obtained under controlled pressure (P) and temperature (T). Longitudinal waves were then produced with piezoelectric transducers at a resonant frequency of 2.68 MHz. The generating transducer sends a burst of sound propagating down the transmission line. At the steel/polymer interface, one part of the energy is transmitted in the polymer; there the pulse travels with a characteristic velocity v, while its amplitude decreases with path length, z, according to the power law $\exp(-\alpha_t z)$, where α_t is the total attenuation resulting from relaxation mechanisms in the polymeric matrix and the scattering phenomenon by fillers. On reaching the second

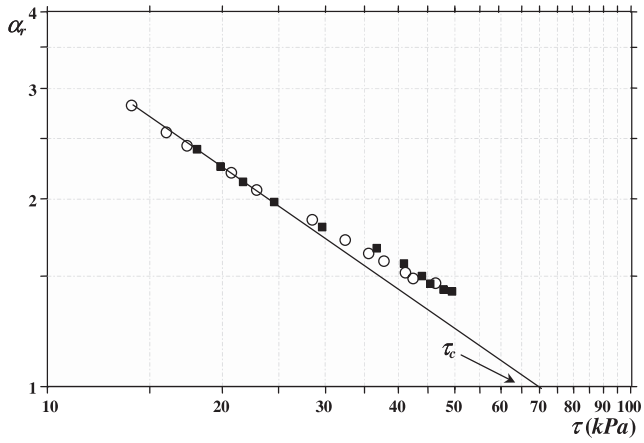

Figure 3. Dimensionless ultrasonic scattering coefficient $\alpha_r = \alpha_{ap}/\alpha_p$ versus the shear stress τ for hydrophilic silica fume fillers in suspension in polypropylene. Filler volume fraction $\phi = 8\%$ (○) or $\phi = 17\%$ (■). $T = 205\,^{\circ}$C.

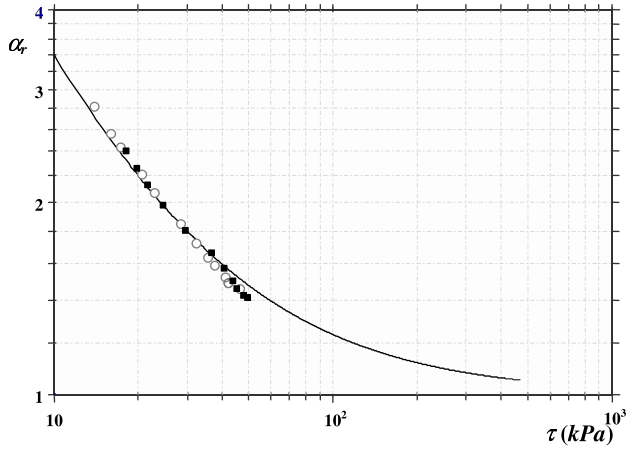

Figure 4. Dimensionless ultrasonic scattering coefficient $\alpha_r = \alpha_{ap}/\alpha_p$ versus the shear stress τ for hydrophilic silica fume fillers incorporated in polypropylene. Filler volume fraction $\phi = 8\%$ (○) or $\phi = 17\%$ (■). $T = 205\,^{\circ}$C. The solid curve is calculated from the power law $\alpha_r \approx 1 + (\tau^*/\tau)^{3m}$ with $m = 1/3$ for rigid clusters.

interface, part of the energy crosses over and is detected by the receiving transducer. The remainder of the energy reverberates in the polymer until completely damped, giving rise to a series of echoes, A_1, A_2, A_3. The ultrasonic attenuation α_t, which measures both the mechanical energy lost to the polymer α_{pol} and the scattering fraction α_{ap} from the fillers, is scaled from the amplitude ratio of successive echoes, and defined on a logarithmic scale in dB as $\alpha_t = \alpha_{ap} + \alpha_{pol} = 10[\log(A_1/A_2)]/e$ [4]. In a second step, the ultrasonic technique was adapted for in-line monitoring [5]. For this purpose, ultrasonic probes were fitted to an extrusion slit die (figure 2(*b*)) to generate ultrasound pulses across the thickness e of the flowing melt (resonant frequency of the ultrasonic transducers $f = 5$ MHz). In this case, the whole polymer flow is characterized at a rate as high as five times per second. The die is also equipped with thermocouples for measuring die temperature T_{die} and melt temperature T_{melt} and pressure sensors to describe the pressure profile along the flow and the pressure P near the ultrasonic probes and the shear stress at the wall. The signals are digitized and the ultrasonic parameters are extracted using specialized high speed signal analysis algorithms [5].

4.4. Shear disruption of hydrophilic silica fume aggregates

We consider in this section shear break-up processes of hydrophilic silica fume particles compounded in polypropylene during extrusion. The screw speed was increased step by step and ultrasonic attenuation was monitored when the steady state was reached, with pressure profiles in the die. Mass throughput measurements were performed to determine the shear rate $\dot{\gamma}$ for each rpm step, using the classical relationship $\dot{\gamma} = 6Q/lh^2$ where Q, l and h are respectively the volume throughput, the width and the thickness of the die. A Rabinovitch-type correction was applied to account for the non-Newtonian behavior of the polymer melt, using the wall shear stress determination from the pressure profile [56]. The die gap was 1 mm and the die temperature was set to 205 °C. To account correctly for the microrheological conditions around the clusters whatever the particle volume fraction, the dimensionless ultrasonic scattering coefficient $\alpha_r = \alpha_{ap}/\alpha_p$ was determined after the dynamical equilibrium state was reached. The flow-dependent changes of the normalized ultrasonic scattering coefficient $\alpha_r(\tau)$ were plotted as a function of the wall shear stress τ (figure 3). Experimental data of the normalized ultrasonic scattering coefficient $\alpha_r(\tau)$ then lie on a single curve, independently of the particle volume fraction, since the local shear stress determines the equilibrium size of interacting aggregates in dense suspension (effective medium approximation) [38, 40]. The low frequency scattering coefficient α_r decreases when increasing the shear stress τ because of the shear break-up of silica fume aggregates into smaller ones. The master curve $\alpha_r(\tau)$ further indicates that correlation effects among individual particles or small aggregates only involve the average particle volume fraction since the transducer cannot resolve aggregates smaller than a voxel [38, 40]. The critical disaggregation shear stress τ_c was then defined in terms of extrapolated intercept [38, 40]. The critical disaggregation shear stress $\tau_c \approx 69 \times 10^4$ N m^{-2} is indeed representative of the mechanical force required to disrupt bonds between silica fume particles [38, 40]. Considering the Derjaguin theory [57], the force $F \approx \tau_c a^2$ which is required to break a bond between two aggregated particles scales as Γa (Γ is the surface adhesive energy). For hydrophilic silica fume particles ($\tau_c \approx 69 \times 10^4$ N m^{-2} and $a \approx 50$ nm), we determine a surface adhesive energy $\Gamma \approx \tau^* a \approx 3.45 \times 10^{-2}$ N m^{-1}. Silica fume aggregates can be considered as rigid clusters of fractal dimension $D \approx 2$ since small elastic deformations are transmitted over the whole structure and preserve the structure of rigidly connected particles in relation to irreversible aggregation [38, 40]. We may thus estimate the dimensionless scattering coefficient $\alpha_r(\tau)$ from the power law (14) with $m = 1/3$. Taking a characteristic shear stress $\tau^* = \tau_c/3$, the power law relationship (14) well describes the shear stress dependence of the dimensionless scattering coefficient $\alpha_r(\tau)$ (figure 4).

4.5. Shear viscosity of hydrophilic silica fume fillers in non-polar liquid medium

We consider in this section the microrheological model proposed by Snabre and Mills [40] based on a reference viscosity law describing the Newtonian behavior of hard spheres in purely hydrodynamic interactions [58, 59]:

$$\frac{\mu(\phi)}{\mu_0} = \frac{1-\phi}{(1-\phi/\phi^*)^2} \tag{15}$$

where μ is the viscosity of the non-aggregated suspension, μ_0 the viscosity of the suspending medium and ϕ^* is the maximum packing fraction of the structural units.

The polymeric fluid further exhibits Newtonian behavior at low shear rates and shear thinning behavior at high shear rates of deformation [60]. We may thus consider the viscoelastic properties of the polymeric matrix by introducing the Bird–Carreau expression in equation (15):

$$\mu_0(\dot\gamma) = \mu_{0\mathrm{m}}[1 + (C\dot\gamma)^2]^{(n-1)/2} \tag{16}$$

where $\mu_{0\mathrm{m}}$ is the zero shear rate viscosity of the matrix polymer and C is a constant related to the onset of shear thinning.

In the case of particle aggregation, the suspension shows a yield stress above the gelation threshold ϕ_g because of the formation of an infinite spanning network which displays a solid-like viscoelasticity behavior. At rest, fractal structures then fill space and reach a maximum size $\hat R(\phi)$, which decreases with particle volume fraction [40]. Above the yield shear stress τ_0, the filling space subclusters of size $\hat R(\phi)$ are broken into smaller clusters and the suspension may flow. The condition $R(\tau) = \hat R(\phi)$ then gives an expression of the yield shear stress τ_0 [40]:

$$\tau_0 \approx \tau^*\left[\left(\frac{\phi}{\phi^*}\right)^{\frac{1}{D-3}} - 1\right]^{-\frac{1}{m}} \qquad \text{for } \phi > \phi_\mathrm{g}. \tag{17}$$

The shear thinning behavior of the flocculated suspension arises from the ability of clusters to screen the shear field and trap the interior fluid. For a fractal dimension $D > 2$, clusters may be considered as impermeable with strong hydrodynamic screening inside the aggregates. Above the yield stress, the finite sized clusters then behave like compact spheres of radius $R(\tau)$ and the viscous dissipation in the fluid between the aggregates determines the effective viscosity of the suspension. Therefore, we may introduce the effective volume fraction ϕ_a of clusters and use the reference viscosity law (equation (15)) to estimate the shear viscosity $(\mu_\mathrm{a}(\phi,\tau)/\mu_0) = (1-\phi_\mathrm{a})/(1-\phi_\mathrm{a}/\phi^*)^2$ of flocculated suspension with $\phi_\mathrm{a}(\tau) = \phi(R(\tau)/a)^{3-D}$ [38, 40].

The effective medium approximation was established from rheo-ultrasonic experiments [8, 38, 40]. As a consequence, we may consider that interacting clusters behave like isolated aggregates in a fluid of viscosity equal to the shear viscosity of the suspension and thus experience an effective shear stress $\tau = \mu_\mathrm{a}(\phi,\tau)\dot\gamma$. Equations (16) and (17) together and the estimate of the shear viscosity of the aggregated suspension with the condition $\tau = \mu_\mathrm{a}(\dot\gamma)\dot\gamma$ then give a non-linear expression of the effective viscosity. For a fractal dimension $D = 2$, the rheological equation then takes the form [40]

$$\sqrt{\tau}\left[1 - \left(\frac{\tau_0}{\tau}\right)^m\right] = \sqrt{\mu\gamma}\left[1 - \frac{\phi}{1-\phi}\left(\frac{\tau^*}{\tau}\right)^m\right]^{1/2} \tag{18}$$

with

$$\mu = \mu_0(\dot\gamma)\frac{1-\phi}{(1-\phi/\phi^*)^2} \tag{19}$$

where τ^* is the critical disaggregation shear stress and μ the viscosity of the dispersed suspension in the high shear regime.

Taking $C = 1.5$, $n = 0.39$ and $\mu_{0\mathrm{m}} = 2.2$ kPa s, the Bird–Carreau model (equation (17)) well describes the shear viscosity of the unfilled PP homopolymer (figure 5). We have further determined the shear viscosity $\mu_\mathrm{a}(\dot\gamma)$ of hydrophilic silica fume fillers in suspension in PP homopolymer. By increasing the shear rate, clusters are progressively broken and the viscosity decreases because of a lower fluid volume fraction trapped in the aggregates. For filler volume fraction close to 0.08, the shear viscosity still exhibits a Newtonian behavior at low shear rates. As the filler volume fraction increases, a yield stress becomes apparent. Viscoelastic properties of the polymeric matrix further dominate the rheological behavior in the higher shear regime (figure 5). Assuming rigid clusters ($m = 1/3$) of fractal dimension $D = 2$ and from the critical shear stress τ^* determined by ultrasonic experiments, we describe the shear thinning behavior of filled PP homopolymer with hydrophilic silica fume particles. The viscosimetric method thus confirms that silica fume aggregates can be considered as rigid clusters. Both the scattering and viscosimetry methods can give an estimate of the disaggregation shear stress τ^* representative of the mechanical force required to disrupt the bonds between particles. However, the critical disaggregation shear stress τ^* determined from rheo-acoustical and viscosimetric experiments differs by a factor of 10. The viscosimetric method likely underestimates

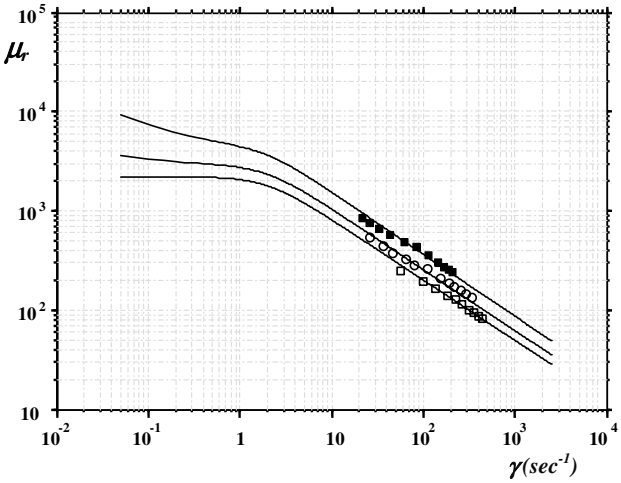

Figure 5. Shear viscosity $\mu_\mathrm{a}(\dot\gamma)$ versus the shear rate $\dot\gamma$ for hydrophilic silica fumes in polypropylene. Filler volume fraction $\phi = 8\%$ (○) or $\phi = 17\%$ (■). The dashed curve represents the viscosity of the unfilled polymer $\phi = 0$ (□). The solid curves are calculated from the microrheological model.

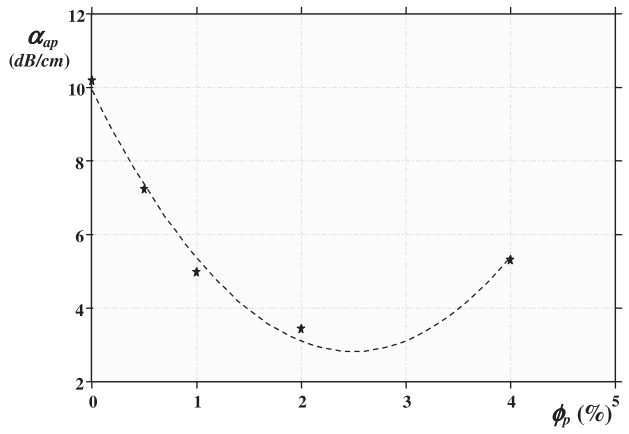

Figure 6. Ultrasonic attenuation α_{ap} (dB cm^{-1}) due to scattering from hydrophilic or partially hydrophobic silica fume aggregates versus the hydrogenated tallow monoalkyl amine concentration $\phi_p(\%)$. $T = 205\,^{\circ}$C and $P = 100$ bar. Filler volume fraction $\phi = 17\%$.

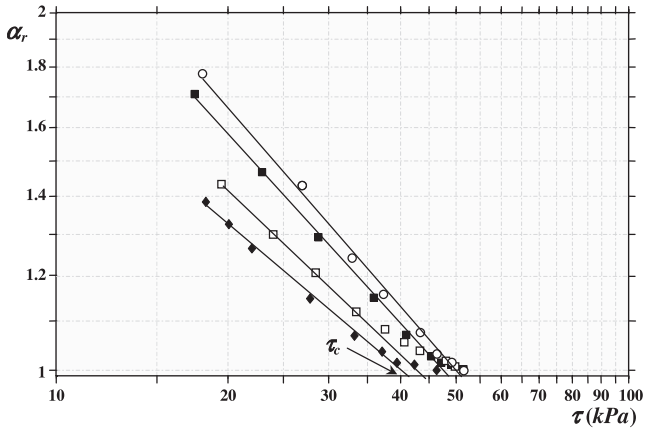

Figure 7. Dimensionless ultrasonic scattering coefficient $\alpha_r = \alpha_{ap}/\alpha_p$ versus the shear stress τ for silica fume fillers treated with hydrogenated tallow monoalkyl amine in polypropylene. Hydrogenated tallow monoalkyl amine concentration $\phi_p = 0.5\%$ (○), $\phi_p = 1\%$ (■), $\phi_p = 2\%$ (□) and $\phi_p = 4\%$ (♦). Filler volume fraction $\phi = 17\%$ and $T = 205\,^{\circ}$C.

the critical disaggregation shear stress τ^* since particle aggregation dominates the rheological behavior in the low shear regime and the shear viscosity is not very sensitive to the presence of small aggregates.

4.6. Equilibrium structure of silica fume fillers in non-polar liquid medium

Rheo-acoustical experiments in the Rayleigh scattering regime provide a way to give a quantitative estimate of particle surface adhesiveness. We explore now the effect of a surface layer of chains grafted onto the silica surface, compounded in non-polar dispersion medium (polypropylene). Static measurements of the low frequency scattering coefficient α_{ap} or flow-dependent changes of the dimensionless ultrasonic scattering coefficient α_r from hydrophilic or partially hydrophobic silica fume aggregates are reported in figures 6 and 7 respectively. Mismatch between the chemical nature of the particle surface containing polar silanol groups (Si–OH) and that of the non-polar liquid medium (polypropylene) favors flocculation of the polar surfaces [25], thus leading to a high ultrasonic scattering coefficient α_{ap} (figure 6). Indeed, hydrophilic silica–silica interactions mainly involve hydrogen bonding between the silanol groups. Such interparticle associations at high filler concentration result in a three dimensional network of flocs and the suspension medium behaves like a physical gel. In contrast, increasing gradually the coating level of hydrogenated tallow monoalkyl amine gives rise to a dense and protective non-polar surface layer on each silica unit, thus inducing a net repulsive pair potential between the fumed silica particles as the excess concentration $\phi_p \approx 2\%$ is raised [25]. In this case, aggregate size is reduced and then the ultrasonic scattering coefficient decreases. Compared to the van der Waals interactions, the steric interaction is much more short ranged and begins to operate only at distances corresponding to the overlap of the surface layers [25]. The steric pair potential involves two separate contributions [25, 44]. For very closely spaced particles, layer molecules cannot adopt all the conformations normally available to them. This effect, called *the volume restriction*, causes a reduction in the degrees of freedom, or loss of entropy, which is equivalent to an increase of the free energy of the system. Such a situation being thermodynamically unfavorable, the system thus tries to evolve in an opposite way to reduce this effect, and the particles tend to move apart [25, 44]. The second contribution arises from a local supersaturation in the region where the adsorbed layers overlap. Indeed, intimate mixing of the chain segments from two different particles can induce repulsion by the *osmotic effect*, which tends to reduce the excess concentration [25, 44]. Under considerations of considerable chain overlapping, the steric pair potential only involves the osmotic contribution and scales as [25]

$$\frac{V_{\text{steric}}}{kT} = \left[\frac{4\pi a}{v_m}\phi_p(L - d/2)^2\right]\left(\frac{1}{2} - \chi\right) \qquad (20)$$

where a is the particle radius, L is the layer thickness, d represents the minimum separation distance between the core particles, k is the Boltzmann constant, T is the absolute temperature, v_m is the volume of a solvent molecule and χ is the Flory–Huggins interaction parameter, which mainly depends upon the solvency of the medium for the chain segments. The term ϕ_p is the average volume fraction of the segments in the grafted layer. Since the term in brackets is always positive, the Flory–Huggins interaction parameter thus determines the sign of the steric pair potential [25]. As shown in equation (20), the repulsion (positive V_{steric}) caused by the osmotic effect is particularly strong if the suspension medium is a good solvent for the grafted chains ($\chi < 1/2$). In this case, chain/solvent interactions predominate and the grafted chains are stretched normal to the silica surface. In contrast, in a poor solvent (negative V_{steric}, $\chi \gg 1/2$), segment/segment interactions predominate as if the particles became sticky. The conformation adopted by the alkyl chains remains flat

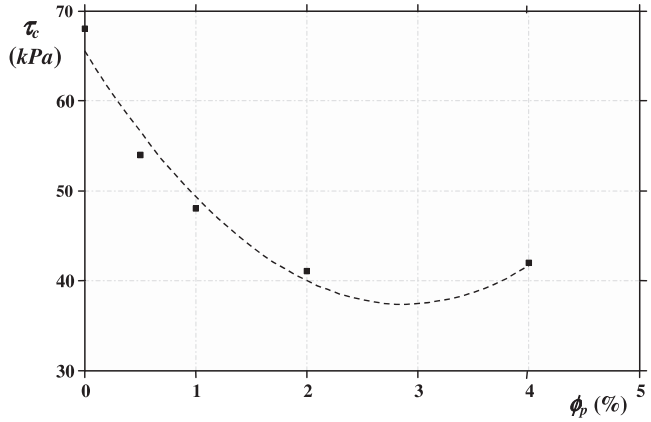

Figure 8. Critical disaggregation shear stresses τ_c determined from rheo-acoustical experiments versus the hydrogenated tallow monoalkyl amine concentration ϕ_p (%).

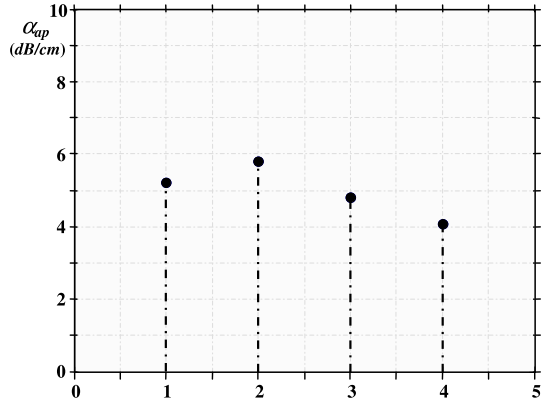

Figure 9. Ultrasonic attenuation α_{ap} (dB cm^{-1}) due to scattering from silica fume fillers treated with monoalkyl chains terminated with the carboxylic acid –COOH (1, $\phi_p = 2\%$; 2, $\phi_p = 4\%$) or hydroxyl group –OH (3, $\phi_p = 2\%$; 4, $\phi_p = 4\%$). $T = 205\,^{\circ}$C and $P = 100$ bar. Filler volume fraction $\phi = 17\%$.

and thus causes the particles to flocculate [25, 44]. One may expect a good miscibility of the hydrogenated tallow monoalkyl amine chains in non-polar dispersion medium such as polypropylene. Indeed, increasing gradually the number of adsorbed chains (without saturating the surface) will cause the growth of the thickness of the adsorbed layer until it becomes greater than $2/\kappa$ ($1/\kappa$ is the Debye length). Loops forming on a particle surface can reach another particle and fix onto it, thereby joining together the two particles. From each particle to its neighbor an aggregate forms by a bridging process. As the excess concentration ϕ_p is raised ($\phi_p \approx 2\%$), each particle is surrounded by a saturated layer of adsorbed chains. The loops fixed onto each particle enter into contact, interact and repel each other, long before the electrostatic repulsion becomes relevant. Furthermore, the use of grafted chains of low molecular weight favors the stabilization of the polymer covered particles [44]. The particles are repulsive at large distances by the electrostatic effect due to the presence of charges at the silica surface and at short distances by the steric repulsion effect [44]. This repulsion may even dominate the van der Waals interactions so that over all distance scales the interparticle forces are repulsive. In this case, the low frequency scattering coefficient α_{ap} representative of the cluster size decreases (figure 6). Considering the flow-dependent changes of the normalized ultrasonic scattering power α_r from the partially hydrophobic silica fume aggregates in polypropylene (figure 7), we have plotted the critical disaggregation shear stress τ_c against the concentration ϕ_p of the tethered chains of hydrogenated tallow monoalkyl amine (figure 8). Surface modification of the silica fume fillers lowers the critical disaggregation shear stress τ_c representative of the particle surface adhesive energy as the excess concentration ϕ_p is raised and thus enhances particle–particle interactions in the polymeric matrix (figure 8).

In contrast, for silica fume fillers treated with monoalkyl chains terminated with the polar carboxylate acid group –COOH in suspension in polypropylene, we observe an increase of the low frequency ultrasonic scattering coefficient α_{ap} as the coating level of the added chains is increased, because of the lower affinity of the carboxylate groups for the

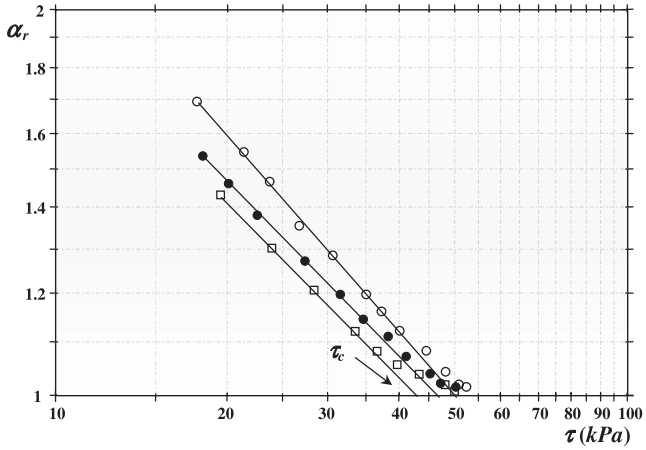

Figure 10. Dimensionless ultrasonic scattering coefficient $\alpha_r = \alpha_{ap}/\alpha_p$ versus the shear stress τ for silica fume fillers treated with monoalkyl chains terminated with the carboxylic acid group –COOH (○, $\phi_p = 2\%$), hydroxyl group –OH (●, $\phi_p = 2\%$) or amino functional group –NH_2 (□, $\phi_p = 2\%$). Filler volume fraction $\phi = 17\%$ and $T = 205\,^{\circ}$C.

silica surface (figure 9). One may expect disorganized multilayers because only one part of the added chains is adsorbed onto the silica surface. The free chain segments orientate their polar head in the less favorable environment and thereby establish contacts with the liquid medium molecules. The miscibility of tethered chains onto the silica surface is then reduced in the less polar continuous medium and the chain segments behave as sticky. In this case, the conformation adopted by the grafted chains is relatively close to the silica surface to minimize interactions with the liquid medium molecules. Stickiness of the surface chains caused by contact dissimilarity with the solvent medium induces an attractive pair potential, which leads to particle flocculation (figure 9) with higher surface adhesive energy compared to silica fume particles treated with monoalkyl chains terminated with the hydroxyl group –OH or the polar amino functional group –NH_2 (figures 9 and 10).

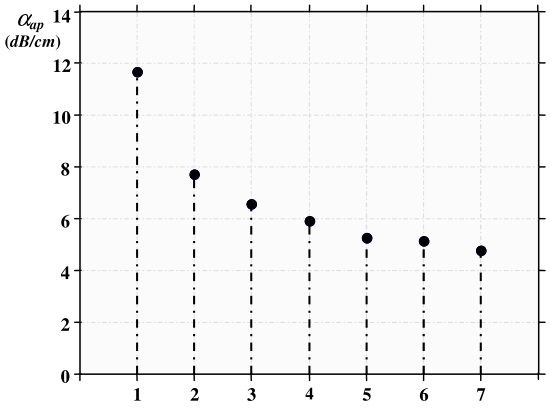

Figure 11. Ultrasonic attenuation α_{ap} (dB cm^{-1}) due to scattering from densified hydrophilic (1) or partially hydrophobic silica fume aggregates in suspension in polypropylene (2, monoalkyl amine $\phi_p = 2\%$; 3, monoalkyl amine $\phi_p = 4\%$; 4, dialkyl amine $\phi_p = 2\%$; 5, dialkyl amine $\phi_p = 4\%$; 6, methyl dialkyl amine $\phi_p = 2\%$; 7, methyl dialkyl amine $\phi_p = 4\%$). $T = 205\,^{\circ}$C and $P = 100$ bar. Filler volume fraction $\phi = 17\%$.

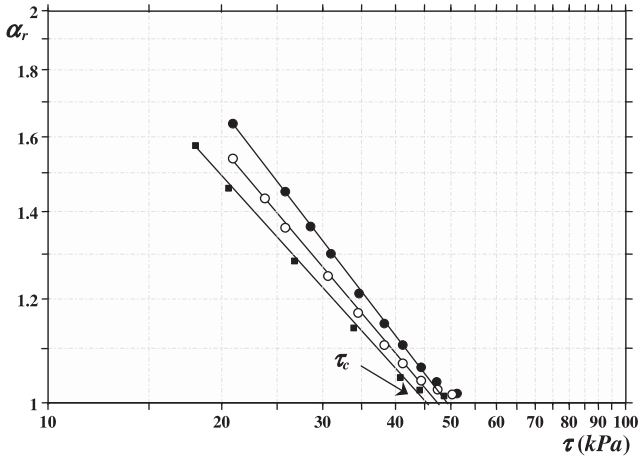

Figure 12. Dimensionless ultrasonic scattering coefficient $\alpha_r = \alpha_{ap}/\alpha_p$ versus the shear stress τ for silica fume fillers treated with hydrogenated tallow monoalkyl amine (●), dialkyl amine (○) or methyl dialkyl amine (■) in polypropylene. Filler volume fraction $\phi = 17\%$ and $T = 205\,^{\circ}$C. Concentration of the grafted chains $\phi_p = 2\%$.

We finally consider surface modification of densified hydrophilic silica fume fillers, performed by grafting monoalkyl amine chains containing the polar amino functional group –NH_2, dialkyl amine derived by substituting one of the hydrogen atoms present in ammonia by the non-polar alkyl chain $(CH_2)_{16}$–CH_3 and methyl dialkyl amine obtained by replacing the last hydrogen in ammonia by the methyl group –CH_3. Interactions of the grafted alkyl chains with the continuous polymer phase predominate for silica fume fillers treated with dialkyl or methyl dialkyl amine compared to silica fume fillers treated with monoalkyl amine and result in a positive free energy of mixing owing to the reduced mismatch in chemical nature between alkyl chains and non-polar liquid medium as the hydrophobic character of the grafted chains increases. A better miscibility of the alkyl chain segments in polypropylene gives rise to a strong net repulsive pair potential as the excess concentration ϕ_p is raised ($\phi_p \approx 4\%$). In this case, the low frequency scattering coefficient α_{ap} decreases (figure 11) and particle–particle interaction is improved as the contact dissimilarity decreases (figure 12).

5. Conclusion

In the present study, shear flow dynamics of polydisperse fractal aggregates in melts of polymeric systems has been investigated by ultrasound scattering. On the basis of the concept of variance in local filler volume fraction and primary particle size distribution of the Rayleigh scatterers described by the gamma probability density function, a rheo-acoustical model for cluster break-up only involving structural parameters (cluster deformability and particle adhesiveness) has been proposed and applied to silica fume aggregates during the extrusion process. Within the framework of fractal flocculation, the normalized ultrasound scattering power from a dense distribution of irreversible Rayleigh polydisperse clusters is nearly isotropic. Far field coherence effects and polydispersity of the scatterers together determine the cluster volume dependence of the dimensionless ultrasonic scattering coefficient without dependence upon the filler volume fraction, fractal dimension of the aggregates or particle size distribution because the ultrasonic wave cannot resolve internal structure of the aggregates smaller than the wavelength. The ultrasound scattering technique presents the main advantage to be only sensitive to cluster volume whatever the internal structure of the clusters. The rheo-acoustical model for cluster break-up well describes the ultrasonic experiments. The flow-dependent changes of the ultrasound scattered power from silica fume clusters well establish the effective medium approximation used in the microrheological models. The shear stress dependence of the dimensionless ultrasonic scattering coefficient further indicates that silica fume aggregates can be considered as rigid clusters ($m = 1/3$) with a fractal dimension $D = 2$, since small elastic deformations are transmitted over the whole structure and then preserves the structure of rigidly connected particles in relation to irreversible aggregation.

Ultrasound scattering technique provides a powerful means for determining the critical disaggregation shear stress in relation to the filler surface modification. From the microrheological model and the quantitative estimate of the critical disaggregation shear stresses, the shear thinning behavior of hydrophilic silica fume clusters in non-polar liquid medium is fairly well described. Miscibility of the grafted chains onto the silica surface is further controlled by the polarity of the solvent medium molecules. Indeed, a good miscibility of the grafted alkyl chain segments onto the silica surface in non-polar dispersion medium such as polypropylene gives rise to a net repulsive pair potential between the silica particles as the excess concentration is raised. As a result, both the aggregate size and the critical disaggregation shear stress representative of the particle surface adhesive energy decrease. In contrast, the stickiness of the surface chains caused by contact dissimilarity with the solvent medium

molecules induces an attractive pair potential which leads to particle flocculation with higher surface adhesive energy.

References

[1] Birley A W, Haworth B and Batchelor J 1992 *Physics of Plastics* (New York: Hanser)
[2] Osswald T A and Menges G 1995 *Materials Science of Polymers for Engineers* (New York: Hanser)
[3] Ferry J D 1961 *Viscoelastic Properties of Polymers* (New York: Wiley)
[4] Piché L, Massines F, Hamel A and Néron C 1988 *US Patent Specification* 4, 754, 645
[5] Piché L, Hamel A, Gendron R, Dumoulin M and Tatibouët J 1995 *US Patent Specification* 5, 433, 112
[6] Alig I, Lellinger D and Joari G P 1992 *J. Polym. Sci.* B **30** 791
[7] Partum M G and Johari J P 1995 *J. Chem. Phys.* **102** 6301
[8] Haïder L, Tatibouët J, Lafaurie A and Ferry L 2002 *J. Phys.: Condens. Matter* **14** 4943–61
[9] Challis R E, Tebbut J S and Holmes A K 1998 *J. Phys. D: Appl. Phys.* **31** 3481–97
[10] Allegra J R and Hawley S A 1971 *J. Acoust. Soc. Am.* **51** 1545–64
[11] Rayleigh J W S 1945 *Theory of Sound* (New York: Dover) pp 414–31
[12] Shung K K, Cloutier G and Lim C C 1992 *IEEE Trans. Biomed. Eng.* **39** 462–9
[13] Hanss M and Boynard M 1979 *Ultrasonic Tissue Characterization II* vol 525, ed M Linzer (Washington: National Bureau of Standard Spec. Publ.) pp 165–9
[14] Lucas R J and Twersky V 1987 *J. Acoust. Soc. Am.* **82** 794–9
[15] Yuan Y W and Shung K K 1988 *J. Acoust. Soc. Am.* **84** 52
[16] Twersky V 1962 *J. Math. Phys.* **3** 700–15
Twersky V 1962 *J. Math. Phys.* **3** 724–34
[17] Twersky V 1978 *J. Acoust. Soc. Am.* **36** 1710–9
[18] Twersky V 1987 *J. Acoust. Soc. Am.* **81** 1609–14
[19] Mo L Y L and Cobbold R S C 1993 *Ultrasonic Scattering in Biological Tissues* ed K K Shung and G A Thieme (Boca Raton, FL: CRC Press) pp 125–71
[20] Angelson B A J 1980 *IEEE Trans. Biomed. Eng.* **27** 61–7
[21] Berger N E, Lucas R J and Twersky V 1991 *J. Acoust. Soc. Am.* **89** 1394–401
[22] Twersky V 1988 *J. Acoust. Soc. Am.* **84** 409–15
[23] Raghavan S R and Khan S A 1995 *J. Rheol.* **39** 1311–25
[24] Raghavan S R, Riley M W, Fedkiw P S and Khan S A 1998 *Chem. Mater.* **10** 244–51
[25] Raghavan R S, Hou J, Baker G L and Khan S A 2000 *Langmir* **16** 1066–77
[26] Jiao W M, Vidal A, Papirer E and Donnet J B 1989 *Colloids Surf.* **40** 279–91
[27] Lee G and Ruppert H 1985 *J. Colloid Interface Sci.* **105** 257–66
[28] Lee G, Murray S and Rupprecht H 1987 *Colloid Polym. Sci.* **265** 535–41
[29] Shirono H, Amano Y, Kawaguchi M and Kato T 2001 *J. Colloid Interface Sci.* **239** 555–62
[30] Chen M and Russel W B 1991 *J. Colloid Interface Sci.* **141** 564–77
[31] Aranguren M I, Mora E, Degroot J V Jr and Macosco C W 1992 *J. Rheol.* **36** 1165–82
[32] Mo L Y L and Cobbold R S C 1992 *IEEE Trans. Biomed. Eng.* **39** 450–61
[33] Haïder L, Boynard M and Snabre P 2003 *Res. Dev. Acoust.* **1** 121–43
[34] Snabre P, Haïder L and Mills P 1999 *Les cahiers de Rhéologie* **XVI** 20–9
[35] Rayleigh J W S 1872 *Proc. Lond. Math Soc.* **4** 253
[36] Mandelbrot B B 1982 *The Fractal Geometry of the Nature* (New York: Freeman)
[37] Witten T A and Sander L M 1981 Diffusion limited aggregation, a kinetic critical phenomena *Phys. Rev. Lett.* **47** 1400–3
[38] Snabre P, Haïder L and Boynard M 2000 *Eur. Phys. J.* E **1** 41–53
[39] Haïder L, Snabre P and Boynard M 2000 *J. Acoust. Soc. Am.* **107** 1715–26
[40] Snabre P and Mills P 1996 *J. Physique* III **6** 1811–34
Snabre P and Mills P 1996 *J. Physique* III **6** 1835–55
[41] Sonntag R C and Russel W B 1987 *J. Colloid Interface Sci.* **115** 378–89
[42] Potanin A A 1993 *J. Colloid Interface Sci.* **157** 399–410
[43] Torres F R, Russel W B and Schowalter W R 1991 *J. Colloid Interface Sci.* **145** 51–73
[44] Daniel J C and Audebert R 1999 *Small Volumes and Larges Surfaces: The Word of Colloids* ed M Daoud and C E Williams (New York: Springer)
[45] De Gennes P G 1987 *Adv. Colloid Interface Sci.* **27** 189
[46] Barthel H, Rosch L and Weis J 1996 Fumed silica: production properties and applications *Organosilicon Chemistry II: From Molecules to Materials* ed N Auner and J Weis (Weinheim: VCH)
[47] *Basic Characteristic of Aerosil* 1993 (*Degussa Technical Bulletin* vol 11) (Akron, OH: Degussa Corp.)
[48] *Aerosil as a Thickening Agent for Liquid Systems* 1993 (*Degussa Technical Bulletin* vol 23) (Akron, OH: Degussa Corp.)
[49] Iler R K 1979 *The Chemistry of Silica* (New York: Wiley-Interscience)
[50] Batteas J D 2000 *Nanotribology Critical Assessment and Future Research Needs* ed S M Hsu (Dordrecht: Kluwer–Academic)
[51] Zhulina E B, Borisov O V and Priamitsyn V A 1990 *J. Colloid Interface Sci.* **137** 495–511
[52] Vincent B 1972 *J. Colloid Interface Sci.* **42** 270–85
[53] Vincent B and Whittington S G 1982 *Polymers at Interfaces and in Disperse Systems* (*Surface and Colloid Science* vol 12) ed E Matjevic (New York: Plenum)
[54] Vincent B 1987 *Colloids Surf.* **24** 269–82
[55] Napper D H 1977 *J. Colloid Interface Sci.* **58** 390–407
[56] Bird R B, Armstrong R and Hassager O 1987 *Dynamics of Polymeric Liquids* vol I *Fluid Mechamics* (New York: Wiley)
[57] Derjaguin B V, Muller V M and Toporov Y P 1975 *J. Colloid Interface Sci.* **53** 314–26
[58] Mills P 1985 *J. Phys. Lett.* **46** L301–9
[59] Mills P and Snabre P 1988 *Rheol. Acta* **26** 105–8
[60] Serra T, Colomer J and Casamitjana X 1997 *J. Colloid Interface Sci.* **187** 466–73